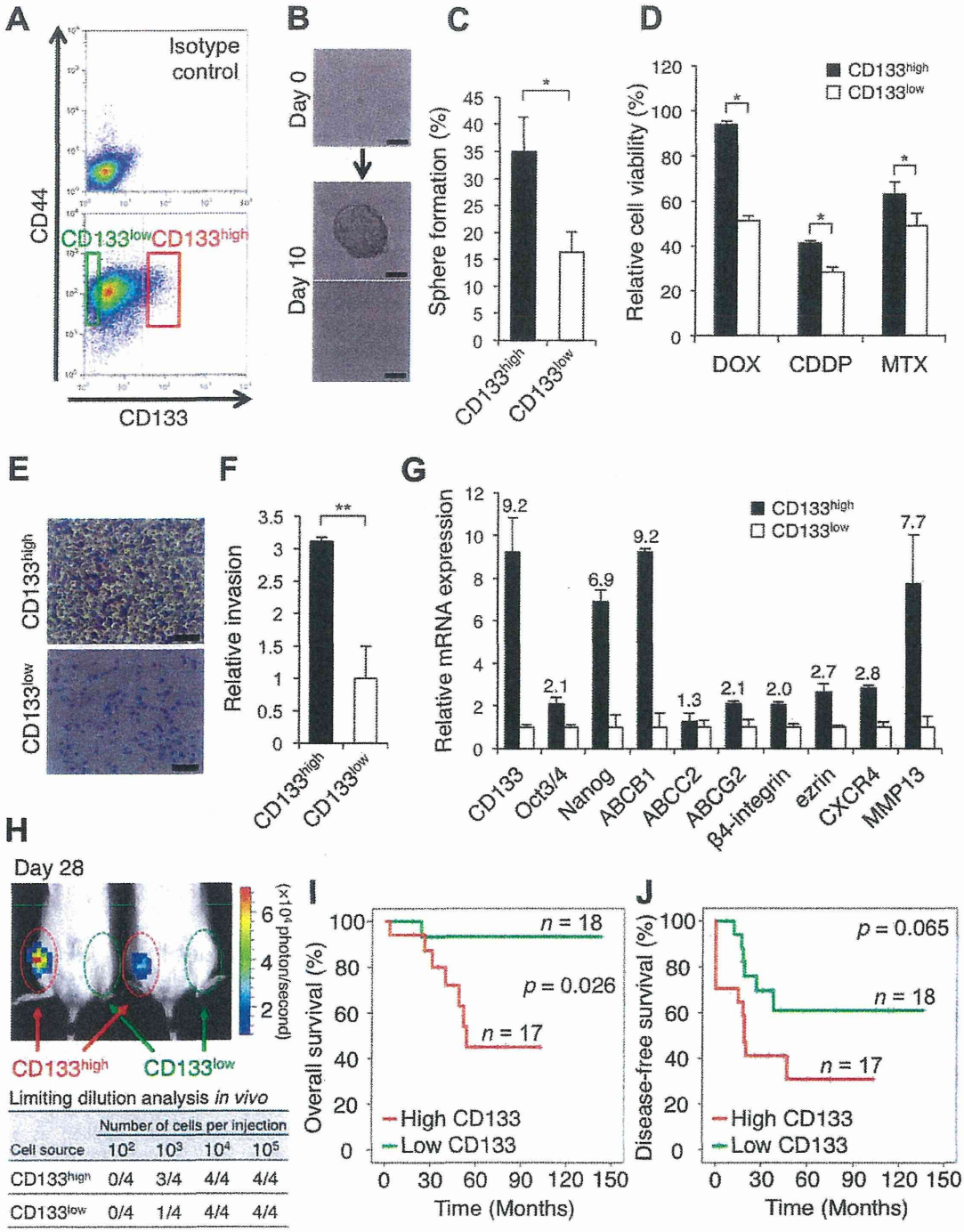

Figure 1. The phenotypic differences and clinical relevance based on the expression of CD133 in osteosarcoma cells. **(A):** The frequency of $CD133^{high}$ cell populations in SaOS2 osteosarcoma cell lines based on fluorescence-activated cell sorting analysis. See also Supporting Information Figure S1A. **(B, C):** Sphere-formation assays using freshly isolated $CD133^{high}$ and $CD133^{low}$ SaOS2 cells. The images were captured on day 10 (B), and the ratios of the wells containing spheres (middle) formed from single cells (top) were counted (C). The wells containing the cells that did not form spheres (bottom) were excluded. Scale bar = 50 μm. Data are presented as mean ± SD ($n = 4$ per group). *, $p < .05$; Student's t test. **(D):** Drug sensitivity of $CD133^{high}$ and $CD133^{low}$ SaOS2 cells. Cell viability after DOX (0.18 μM), CDDP (2.5 μM), or MTX (0.08 μM) treatment was analyzed. Data are presented as mean ± SD ($n = 3$ per group). *, $p < .05$; Student's t test. **(E, F):** Invasion assays in $CD133^{high}$ and $CD133^{low}$ SaOS2 cell populations ($n = 3$ per group). The number of invaded cell were photographed (E) and counted (F). Data are presented as mean ± SD ($n = 3$ per group). **, $p < .01$; Student's t test. Scale bar = 200 μm. **(G):** Quantitative polymerase chain reaction analysis of stem cell-associated, multiple drug-resistant transporters, and metastasis-associated genes of $CD133^{high}$ and $CD133^{low}$ SaOS2 cell populations. β-Actin was uses as an internal control. Data are presented as mean ± SD ($n = 3$ per group). **(H):** Limiting dilution analysis of $CD133^{high}$ (red circles) and $CD133^{low}$ (green circles) SaOS2-luc cell populations *in vivo*. Both cell populations were injected orthotopically into mice ($n = 4$ per group). The upper figure represents the tumor formation in mice from 1×10^3 cells of $CD133^{high}$ cells. The lower table shows the number of mice that developed tumors from various numbers of $CD133^{high}$ or $CD133^{low}$ cells. The tumor growth from $CD133^{high}$ cells was observed in 0/4 mice at 10^2 cells, 3/4 mice at 10^3 cells, 4/4 mice at 10^4 cells, and 4/4 mice at 10^5 cells, while those from $CD133^{low}$ cells was observed in 0/4 mice at 10^2 cells, 1/4 mice at 10^3 cells, 4/4 mice at 10^4 cells, and 4/4 mice at 10^5 cells. **(I, J):** The Kaplan-Meier curves for overall survival (I; $p = .026$; log-rank test) and disease-free survival (J; $p = .065$, log-rank test) based on the level of CD133 expression in the biopsy specimens from 35 osteosarcoma patients. See also Supporting Information Figure S2A and Table S1. Abbreviations: CDDP, cisplatin; DOX, doxorubicin; MTX, methotrexate.

chemotherapeutic agents that are used against osteosarcoma. The $CD133^{high}$ cells were more resistant to these chemotherapeutics than $CD133^{low}$ cells (Fig. 1D). In addition, $CD133^{high}$ cells showed a higher invasive ability than $CD133^{low}$ cells (Fig. 1E, 1F). Performing qRT-PCR reactions on mRNA from freshly isolated $CD133^{high}$ and $CD133^{low}$ cells revealed that $CD133^{high}$ SaOS2 cells expressed higher levels of *Oct3/4* and *Nanog*, which are essential transcription factors that play critical roles in the self-renewal and pluripotency of embryonic stem cells (Fig. 1G) [15–17]. Meanwhile, the expression levels of the genes that are essential for differentiation, such as *Runx2*, *Osterix*, and *Sox9* [33–36], were lower in $CD133^{high}$ than in $CD133^{low}$ cells (Supporting Information Fig. S1C). In addition, the multidrug resistance transporter genes *ABCB1*, *ABCC2*, and *ABCG2* and the metastasis-associated genes *β4-integrin*, *ezrin*, *MMP-13*, and *CXCR4* [30, 37] were upregulated in $CD133^{high}$ cells relative to $CD133^{low}$ cells (Fig. 1G). Importantly, the $CD133^{high}$ SaOS2 cells showed stronger tumorigenicity *in vivo* than the $CD133^{low}$ SaOS2 cells (Fig. 1H). We identified tumor initiation on the right legs of three in four mice transplanted with 1×10^3 $CD133^{high}$ cells but only one in four mice formed tumor with 1×10^3 $CD133^{low}$ cells on the left legs. To evaluate the clinical importance of CD133 expression, cell lines established from fresh human osteosarcoma biopsies were analyzed by flow cytometry, and these cell lines contained a low proportion ($< 10\%$) of $CD133^{high}$ cells (Supporting Information Fig. S1B). Furthermore, a clinical study of 35 osteosarcoma patients revealed that high expression levels of CD133 mRNA were associated with significantly worse survival rates among osteosarcoma patients (Fig. 1I, 1J; Supporting Information Figure S2A). In this study, all biopsy samples from patients who developed lung metastasis at first diagnosis represented high expression level of CD133 ($p = .045$; Supporting Information Table S1), suggesting that the expression of CD133 closely correlate with osteosarcoma metastasis. Collectively, the osteosarcoma $CD133^{high}$ cell population possessed highly malignant phenotypes, and the expression of CD133 revealed a prognostic value of osteosarcoma patients.

MiR-133a Functions as a Key Regulator of Malignant Phenotypes in Osteosarcoma

Following the confirmation of the malignant phenotypes in the osteosarcoma $CD133^{high}$ population, we further characterized the molecular mechanisms underlying these phenotypes. We focused on miRNAs because of their ability to simultaneously regulate multiple pathways responsible for the malignant phenotypes by targeting multiple genes. miRNAs are small, regulatory RNA molecules that modulate the post-transcriptional expression of their target genes and play important roles in a variety of physiological and pathological processes, including tumor biology [23, 25, 38]. miRNA expression profiling has become a useful diagnostic and prognostic tool, and many studies have indicated that miRNAs act as either oncogenes or tumor suppressors [38]. In our miRNA microarray analysis of isolated $CD133^{high}$ and $CD133^{low}$ cells using 866 sequence-validated human miRNAs, we identified 20 miRNAs that were upregulated in $CD133^{high}$ cells and additional qRT-PCR analysis demonstrated that the expression levels of miR-1 and miR-10b, together with miR-133a, which represents the "miR-1 cluster" transcribed from adjacent miR-1 genes, were consistent with the microarray data (Fig. 2A; Supporting Information Fig. S3A, Table S8). Indeed, miR-1 and miR-133a are physically linked, and both the miR-1-1/miR-133a-2 (chromosome 20q13.33) as well as miR-1–2/miR-133a-1 clusters (chromosome 18q11.2) are present. miR-10b is embedded in the *HOX* gene cluster and maps between the *HOXD3* and *HOXD4* genes on chromosome 2q31. Since miR-10a and miR-133b would presumably be functionally redundant to miR-10b and miR-133b, respectively, we also confirmed that miR-133b, but not miR-10a, was upregulated in $CD133^{high}$ cell population (Supporting Information Fig. S3B).

To determine whether these miRNAs could regulate the malignant phenotypes of osteosarcoma, we manipulated the expression levels of miR-1, 10b, and 133a in $CD133^{low}$ cells (Supporting Information Fig. S4A). These miRNAs, especially miR-133a, enhanced the invasiveness of $CD133^{low}$ cells compared with control oligos (Fig. 2B, 2C). Interestingly, the combined transfection of all of these miRNAs enhanced the invasiveness of $CD133^{low}$ cells to the greatest extent (Fig. 2C). However, the transfection of miR-133a did not increase the mRNA level of CD133 (Supporting Information Fig. S4B), suggesting that miR-133a does not affect the expression of the molecules upstream of CD133. These results indicated that miR-133a simultaneously regulate several molecular pathways that are associated with cell invasion of the malignant cell population within osteosarcoma. In our experiment using fresh clinical samples, miR-133a expression was also high in the $CD133^{high}$ fraction of osteosarcoma biopsies (Fig. 2D). Surprisingly, a clinical study based on qRT-PCR using clinical FFPE samples revealed that the high expression of miR-133a closely correlated with a poor prognosis of osteosarcoma patients (log-rank test, $p = .032$ for overall survival, $p = .081$ for disease-free survival; Fig. 2E, 2F; Supporting Information Fig. S2B, Table S2).

Silencing of MiR-133a Inhibits the Cell Invasion of $CD133^{high}$ Osteosarcoma Cell Population

To evaluate whether silencing of miR-133a show the therapeutic effect on osteosarcoma cells, we manipulated the expression of miR-133a by introducing LNAs. LNAs are a class of nucleic acid analogs that possess a very high affinity and excellent specificity toward complementary DNA and RNA, and LNA oligonucleotides have been applied as antisense molecules both *in vitro* and *in vivo* [39–41]. The SaOS2 $CD133^{high}$ cell population was isolated by cell sorting and was then transfected with LNA-antimiR-133a (LNA-133a) and LNA-NC. As a control, the isolated SaOS2 $CD133^{low}$ cell population was also transfected with LNA-NC. Prior to functional assay, we confirmed the efficacy of LNA-133a using both qRT-PCR analysis and a sensor vector which allowed us to measure the suppressive effect of LNA by luciferase assay (Supporting Information Fig. S5A–S5D). We observed that the LNA-133a-treated SaOS2 $CD133^{high}$ cells demonstrated decreased invasiveness relative to LNA-NC-treated $CD133^{high}$ cells, whereas there was no significant difference of cell proliferation between the two populations (Fig. 2G, 2H; Supporting Information Fig. S5E). These observations suggest that silencing of miR-133a in $CD133^{high}$ cells could reduce the cell invasion of the malignant cell population within osteosarcoma tissue.

©AlphaMed Press 2013

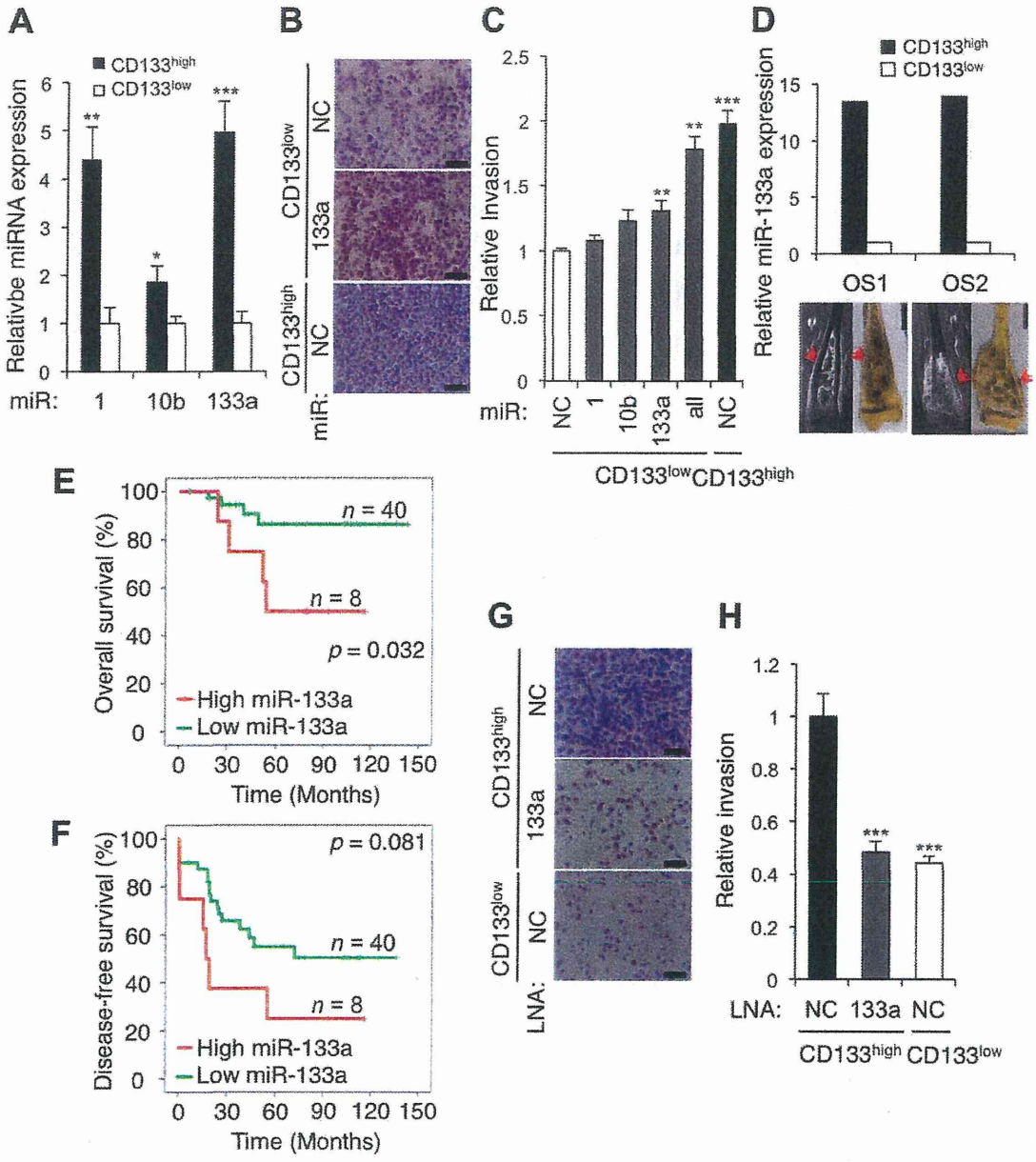

Figure 2. MiR-133a regulates cell invasion of tumor-initiating cell population within osteosarcoma and represents prognostic value. **(A):** The upregulated expression levels of miR-1, 10b, and 133a in CD133^{high} cell population. Data are presented as mean ± SD ($n = 3$ per group). *, $p < .05$; **, $p < .01$; ***, $p < .001$; Student's t test. **(B, C):** Invasion assays in purified CD133^{low} SaOS2 cells transfected with miR-1, 10b, and 133a oligos. CD133^{low} SaOS2 cell populations were transfected with miR-1, 10b, 133a, or NC mimics at a final concentration of 30 nM. At the time periods of 24 hours post-transfection, cells were seeded and cultured on the invasion chamber for 36 hours. The number of invaded cell were photographed (B) and counted (C). Scale bar = 200 μm. Data are presented as mean ± SD ($n = 3$ per group). **, $p < .01$; ***, $p < .001$, calculated with one-way ANOVA with Bonferroni's multiple comparison when compared with the CD133^{low} cell population treated with miR-NC. **(D):** The expression level of miR-133a in CD133^{high} and CD133^{low} populations of freshly resected patient biopsies. **(E, F):** The Kaplan-Meier curves for overall survival (E) and disease-free survival (F) based on the levels of miR-133a expression in 48 formalin-fixed paraffin-embedded tissues from osteosarcoma biopsy specimens, as determined using quantitative reverse transcriptase polymerase chain reaction. The overall survival rate ($p = .032$; log-rank test) and disease-free survival rate ($p = .081$; log-rank test) for osteosarcoma patients with high miR-133a expression (red line) were compared with those for patients with low miR-133a expression (green line). See also Supporting Information Figure S2B and Table S2. **(G, H):** Invasion assays in LNA-133a-treated SaOS2 CD133^{high} populations. CD133^{high} and CD133^{low} SaOS2 cell populations were isolated and transfected with LNA-133a or LNA-NC to reduce the expression of miR-133a in the CD133^{high} cell population. As a control, CD133^{low} cell populations were transfected with LNA-NC. At the time periods of 24 hours post-transfection, cells were seeded and cultured on the invasion chamber for 36 hours. The number of invaded cell were photographed (G) and counted (H). Scale bar = 200 μm. Data are presented as mean ± SD ($n = 3$ per group). ***, $p < .001$, calculated with one-way ANOVA with Bonferroni's multiple comparison when compared with the CD133^{high} cell populations treated with LNA-NC. Abbreviations: LNA, locked nucleic acid; NC, negative control.

©AlphaMed Press 2013

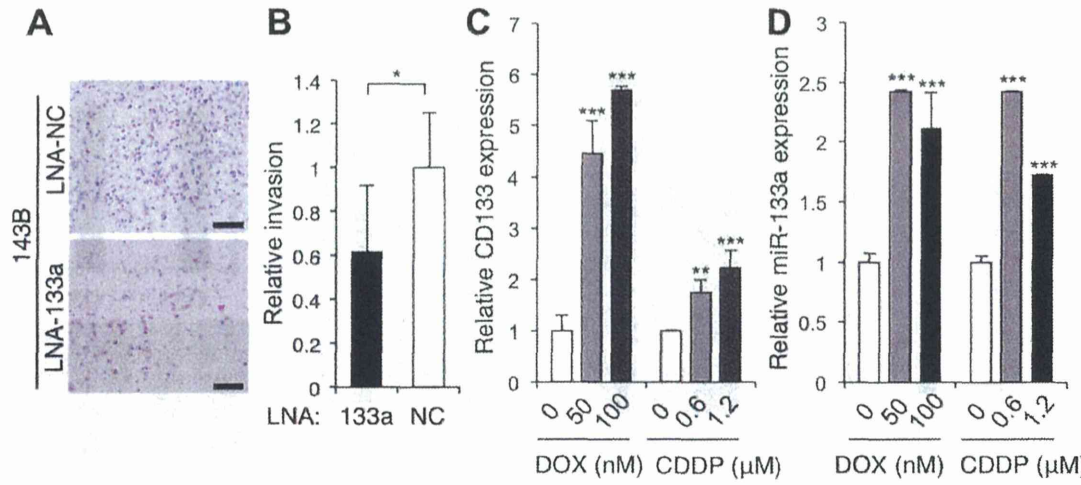

Figure 3. Chemotherapy induces the expression of miR-133a in highly malignant osteosarcoma 143B cells. **(A, B):** Invasion assay in highly metastatic osteosarcoma 143B cells treated with LNA-133a and NC. At the time periods of 24 hours post-transfection, cells were seeded and cultured on the invasion chamber for 24 hours. The number of invaded cell were photographed (A) and counted (B). Scale bar = 200 μm. Data are presented as mean ± SD ($n = 3$ per group). *, $p < .05$; Student's t test. **(C):** The induced expression of CD133 in 143B cells in the presence of chemotherapeutics (DOX and CDDP, 48 hours). Data are presented as mean ± SD ($n = 3$ per group). **, $p < .01$; ***, $p < .001$, calculated with one-way ANOVA with Bonferroni's multiple comparison when compared with untreated cells. **(D):** The induced expression of miR-133a in 143B cells in the presence of chemotherapeutics (DOX and CDDP, 48 hours). Data are presented as mean ± SD ($n = 3$ per group). ***, $p < .001$, calculated with one-way ANOVA with Bonferroni's multiple comparison when compared with untreated cells. Abbreviations: CDDP, cisplatin; DOX, doxorubicin; LNA, locked nucleic acid; NC, negative control.

The Expression Levels of MiR-133a in Osteosarcoma Cells Are Enhanced by Chemotherapy

Next, we validated the efficacy of LNA-133a on highly malignant metastatic osteosarcoma 143B cells, since SaOS2 cells represent low metastatic ability *in vivo* [42, 43]. Meanwhile, we needed to evaluate the efficacy of LNA on "bulk" 143B cells, assuming clinical situations. As a result, LNA-133a reduced the invasiveness of 143B cells (Fig. 3A, 3B) but did not influence cell proliferation (Supporting Information Fig. 5F). Since recent study has indicated a novel mechanism of chemotherapy-induced tumor progression via expansion of TIC population [44], the expression levels of CD133 and the related miR-133a within cells treated with or without chemotherapeutics were analyzed. As a result, we observed that the expression levels of miR-133a, together with CD133, were enhanced by chemotherapy. qRT-PCR analysis revealed that DOX-treated or CDDP-treated (2 days) 143B cells expressed higher levels of CD133 and miR-133a compared with untreated 143B cells (Fig. 3C, 3D). Therefore, silencing of miR-133a before or during chemotherapy may prevent the increased expression of miR-133a, which enhanced the malignant phenotypes and was induced by chemotherapeutics.

Therapeutic Administration of LNA-133a with Chemotherapy Inhibits Spontaneous Lung Metastasis and Prolongs the Survival of Osteosarcoma-Bearing Mice

To extend our *in vitro* findings and to determine whether silencing of miR-133a could be an effective therapeutic option for osteosarcomas, we next examined the effect of LNA-133a on a spontaneous lung metastasis model of osteosarcoma. Experimentally, 1.5×10^6 143B cells transfected with the firefly luciferase gene (143B-luc) were implanted orthotopically into the right proximal tibia of athymic nude mice. The implanted tumor growth and the presence of distant metastases were analyzed weekly for luciferase bioluminescence using an *in vivo* imaging system. We used a new treatment protocol (Fig. 4A) with the intravenous (i.v.) administration of LNA-133a (10 mg/kg) 24 hours before intraperitoneal (i.p.) injection of CDDP (3.5 mg/kg) to prevent the induction of malignant phenotypes by chemotherapy, which were indicated in the *in vitro* experiments. Prior to conducting these animal studies, we confirmed that miR-133a levels were reduced in osteosarcoma tissues from LNA-133a-treated mice compared with control mice (Supporting Information Fig. S6A, S6B). To assess the efficacy of our protocol, the results were compared with the results obtained for the following four control groups ($n = 10$ per group): the control saline followed by control saline group, the LNA-NC followed by control saline group, the LNA-133a followed by control saline group, and the LNA-NC followed by CDDP group. After implantation of the 143B-luc cells, five mice within each one cage were sacrificed at 3 weeks after evaluating lung metastasis by *in vivo* imaging and validated for lung metastasis formation by additional *in vivo* imaging and histological examination of the lung, whereas the other five mice in the other cage were evaluated for survival periods. The results demonstrated that the tumor expression levels of miR-133a were decreased in the presence of LNA-133a (Fig. 4B). Although tumor growth at the primary site was significantly reduced in CDDP-treated group, we identified no significant difference between LNA-133a-CDDP-treated mice and LNA-NC-CDDP-treated mice (Fig. 4C, 4D). We observed lung metastases on day 22 in nine (90%) saline-saline-treated mice, eight (80%) LNA-NC-saline-treated mice, seven (70%) LNA-133a-saline-treated mice, eight (80%) LNA-NC-CDDP-treated mice, and three (30%) LNA-133a-CDDP-

©AlphaMed Press 2013

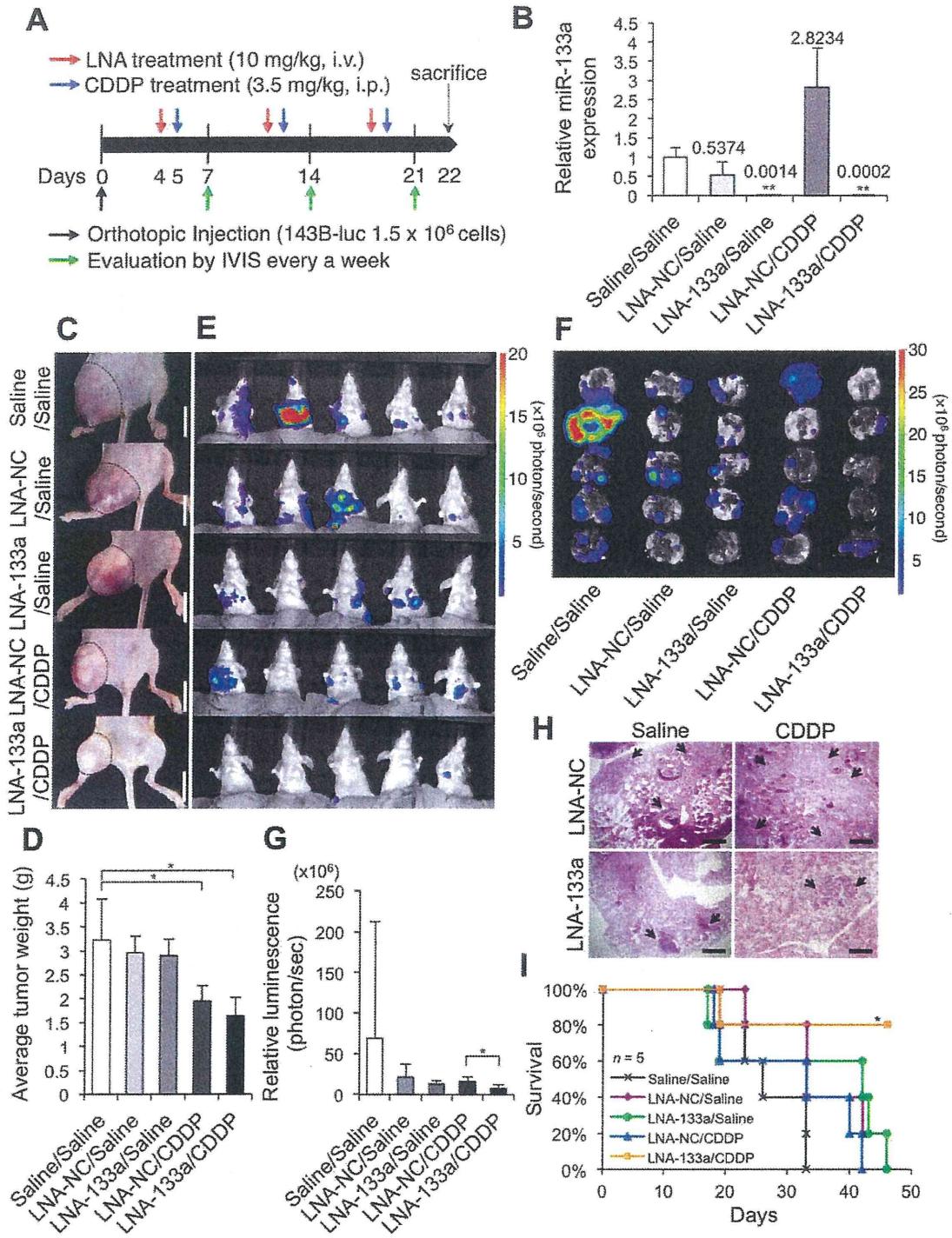

Figure 4. Therapeutic administration of LNA-133a with systemic chemotherapy inhibits osteosarcoma progression *in vivo*. **(A):** A schematic representation of the LNA-133a (red arrow) and CDDP (blue arrow) administration schedule for 143B-luc-bearing mice. **(B):** The expression levels of miR-133a in osteosarcoma tissues ($n = 5$ per group) analyzed by quantitative reverse transcriptase polymerase chain reaction. The tumors were obtained during autopsy after completion of treatment on day 22. Data are presented as mean ± SD ($n = 5$ per group). **, $p < .01$, as compared to control saline-treated group; Student's t test. **(C, D):** Tumors at the primary site of each treatment group measured on day 22. The macroscopic appearances of 143B-luc tumors in each group of mice on day 22 are shown (C). The tumor masses outlined by a dotted line. Scale bar = 10 mm. The 143B-luc tumors from each group of mice were weighed on day 22 (D). Data are presented as mean ± SD ($n = 5$ per group). *, $p < .05$, as compared to control saline-treated group; Student's t test. **(E–G):** The lung metastases of each treatment group measured on day 22 using an IVIS. The representative luminescence of the chest regions in each group of mice was determined (E). For each mouse that was sacrificed to validate the lung metastases, each lung was re-evaluated using IVIS (F). The representative average luminescence of the chest region in each group of mice ($n = 10$) was compared among the treatment groups (G). Data are presented as mean ± SD ($n = 5$ per group). *, $p < .05$, as compared with LNA-NC/CDDP and LNA-133a/CDDP group; Student's t test. **(H):** Lung metastases validated by H&E staining. Black arrow represents metastatic foci in the lung. Scale bars = 500 μm. **(I):** Survival curves for each group of mice by Kaplan-Meier analysis. Log-rank test was performed between LNA-NC/CDDP group (blue line) and LNA-133a/CDDP group (red line) (*, $p = .026$). Abbreviations: CDDP, cisplatin; IVIS, *in vivo* imaging system; LNA, locked nucleic acid; NC, negative control.

treated mice ($n = 10$; Fig. 4E, 4F). We observed the decreased signal intensity in the chest regions of LNA-133a-CDDP-treated mice compared to those of LNA-NC-CDDP-treated mice (Fig. 4G). Both the number and size of lung metastases were validated by histopathological examination (Fig. 4H). We found low cell concentration in lung metastatic foci of CDDP-treated groups, indicating therapeutic effect of chemotherapy, and identified smallest number of osteosarcoma metastatic foci in the lung of LNA-133a-CDDP-treated mice. Furthermore, LNA-133a-CDDP-treated mice showed longest survival periods among the five groups in Kaplan-Meier analysis (log-rank test, $p = .026$; Fig. 4I). Despite the conserved sequence of mature hsa-miR-133a and mmu-miR-133a (Supporting Information Fig. S7A), all mice exhibited minimal toxic effects on various tissues, including the heart, liver, skeletal muscle, and blood test, during the observation period (Supporting Information Fig. S7B–S7H, S8A–S8I). Thus, systemic administration of LNA-133a was effective for the suppression of lung metastases in a xenograft model of a highly metastatic osteosarcoma in the presence of CDDP.

Multiple Target Genes of MiR-133a Function as Regulators of Cell Invasion and Closely Correlate with Clinical Behavior of Osteosarcoma

We demonstrated that miR-133a regulated the malignancy of $CD133^{high}$ osteosarcoma cell population and that silencing of miR-133a expression with chemotherapeutics inhibited the osteosarcoma metastasis *in vivo*. Next, to understand the molecular mechanism regulated by miR-133a in the tumor-initiating population, we performed mRNA expression profiling using two different microarray analyses together with *in silico* predictions (Supporting Information Fig. S9A). We detected 1,812 genes that were downregulated by at least 1.2-fold in the first microarray analysis, which was performed from total RNA collected from SaOS2 $CD133^{low}$ cells transduced with miR-133a or NC. Furthermore, 4,976 genes were upregulated by at least 2-fold in the second microarray analysis of mRNA expression using RNA collected using anti-Argonaute 2 antibody immunoprecipitation (Ago2 IP) in $CD133^{low}$ cells transduced with miR-133a or NC. Subsequently, 226 genes were collected using both methods, and 20 genes were identified in TargetScanHuman 6.0, a publicly available *in silico* database (Fig. 5A). Overall, 10 putative miR-133a target genes were selected from these combined data, and we reduced the expression of these molecules using an siRNA-induced gene knockdown system to investigate whether these candidates are functionally important targets of miR-133a in osteosarcoma cells. As a result, the knockdown of four genes (*SGMS2*, *UBA2*, *SNX30*, and *ANXA2*) enhanced the invasiveness of $CD133^{low}$ SaOS2 cells (Fig. 5B). To validate whether these molecules are regulated by miR-133a, we cloned the 3′ UTR fragment (Fig. 5C) containing the putative miR-133a binding sites downstream of a luciferase coding sequence and performed cotransfection of the luciferase reporter and miR-133a oligos in SaOS2 cells. Luciferase activity levels were reduced by approximately 36%–55% in the cells cotransfected with miR-133a compared with the cells cotransfected with the NC oligos (Fig. 5D). Consequently, *SGMS2*, *UBA2*, *SNX30*, and *ANXA2* functioned as direct targets of miR-133a. Indeed, these molecules have been suggested to have antitumor function in the other types of tumors [45–47]. Among them, *ANXA2* is downregulated in osteosarcoma metastases compared to primary site [48]. The expression levels of these targets were decreased in $CD133^{high}$ cells (Supporting Information Fig. S9B) and reduced via miR-133a upregulation in $CD133^{low}$ cells (Supporting Information Fig. S9C). The increased expression levels of the targets after silencing of miR-133a were confirmed by immunohistochemistry of LNA-treated tumors and qRT-PCR (Fig. 5E, 5F; Supporting Information Fig. S9D). Taken together, LNA-133a was found to inhibit cell invasion of the malignant cell population of osteosarcoma through multiple molecular pathways. Finally, we observed a strikingly close correlation between these mRNA expression levels of the miR-133a targets and osteosarcoma patient prognosis (Fig. 6A–6D). Patients with higher expression levels of these targets significantly survived longer than those with lower expression levels. These results would support the importance of regulating the expression of miR-133a during current osteosarcoma treatment, providing insight into the development of more effective therapies against osteosarcoma.

Discussion

Cancer researchers today are confronted with how to overcome the natural resistance and the acquired resistance of cancer cells within tissue, despite the many cancer treatment options. The CSC or TIC hypothesis has been an attractive model to account for the functional heterogeneity that is commonly observed in solid tumors [7]. To characterize and eliminate the malignant cells in cancers that follow this model, it has been necessary to focus on the small subpopulations of tumorigenic cells [49]. Tremendous efforts and evidence have accumulated to identify these subpopulations [13–18, 20, 21]. However, these markers are generally difficult to be targeted because of their distribution on the normal stem cells. For example, targeting CD133 seems unsafe because this cell-surface protein is primarily expressed in stem and progenitor cells [50] such as the embryonic epithelium [51], brain stem cells [52], and hematopoietic stem cells [32, 53]. Therefore, the molecular mechanisms underlying the malignant phenotypes must be elucidated to avoid toxicities, which have not been fully accomplished. On the basis of our results, we propose novel therapeutic strategies, beyond the use of traditional antiproliferative agents, for suppression of the highly malignant cell population within osteosarcoma using RNAi therapeutics, which is expected to be the "next-generation" anticancer strategy. Subsequently, we present four novel discoveries that were identified in a preclinical trial of novel therapeutic strategies against osteosarcoma.

First, we identified human miR-133a as a key regulator of the malignant tumor-initiating phenotypes of osteosarcoma. The other miRNAs that might regulate these phenotypes included miR-1 and miR-10b. The human miRNA hsa-miR-10b is also positively associated with high-grade malignancies, including breast cancer [54, 55], pancreatic adenocarcinomas [56], and glioblastomas [57]. However, the importance of miR-10b in sarcoma development has not been previously reported. In our experiment, miR-10b regulated, less than miR-133a, the cell invasion of osteosarcoma. The human miRNAs hsa-miR-1 and hsa-miR-133a are located on the same chromosomal region in a so-called cluster. We found that miR-

©AlphaMed Press 2013

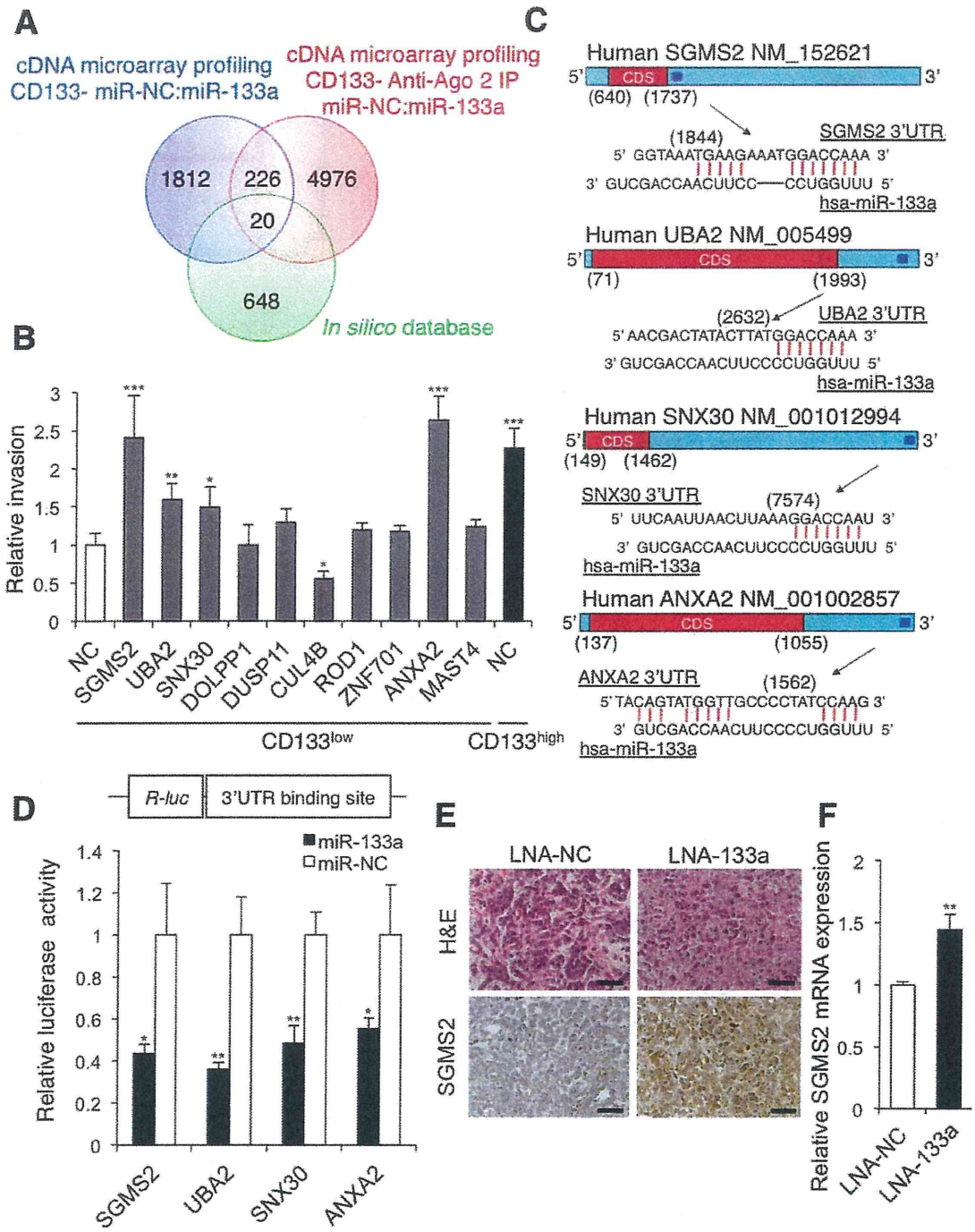

Figure 5. The direct target genes of miR-133a regulate malignant phenotypes of osteosarcoma. **(A):** A Venn diagram of the candidate target mRNAs of miR-133a based on the cDNA microarrays and *in silico* database. **(B):** Invasion assays performed using SaOS2 cells 24 hours post-transfection of the 10 siRNAs. $CD133^{high}$ and $CD133^{low}$ SaOS2 cell populations were isolated using flow cytometry and transfected with 10 siRNAs against the identified genes in **(A)**. Data are presented as mean ± SD ($n = 3$ per group). *, $p < .05$; **, $p < .01$; ***, $p < .001$, calculated with one-way ANOVA with Bonferroni's multiple comparison when compared with the $CD133^{low}$ cells transfected with nontargeting siRNA. **(C):** Schematics of the miR-133a binding site within the 3′ UTR of the target mRNAs. **(D):** Luciferase activities measured by cotransfecting miR-133a oligos and the luciferase reporters. Data are presented as mean ± SD ($n = 3$ per group). *, $p < .05$; **, $p < .01$; Student's *t* test. **(E, F):** Representative SGMS2 immunohistochemistry images of 143B-luc tumor sections (E) and the relative SGMS2 expression of 143B-luc tumor sections performed by quantitative reverse transcriptase polymerase chain reaction analysis (F). Scale bars = 50 μm. Data are presented as mean ± SD ($n = 3$ per group). **, $p < .01$; Student's *t* test. Abbreviations: ANXA2, annexin A2; IP, immunoprecipitation; LNA, locked nucleic acid; NC, negative control; SGMS2, sphingomyelin synthase 2; SNX30, sorting nexin family member 30; UTR, untranslated region; UBA2, ubiquitin-like modifier activating enzyme 2.

©AlphaMed Press 2013

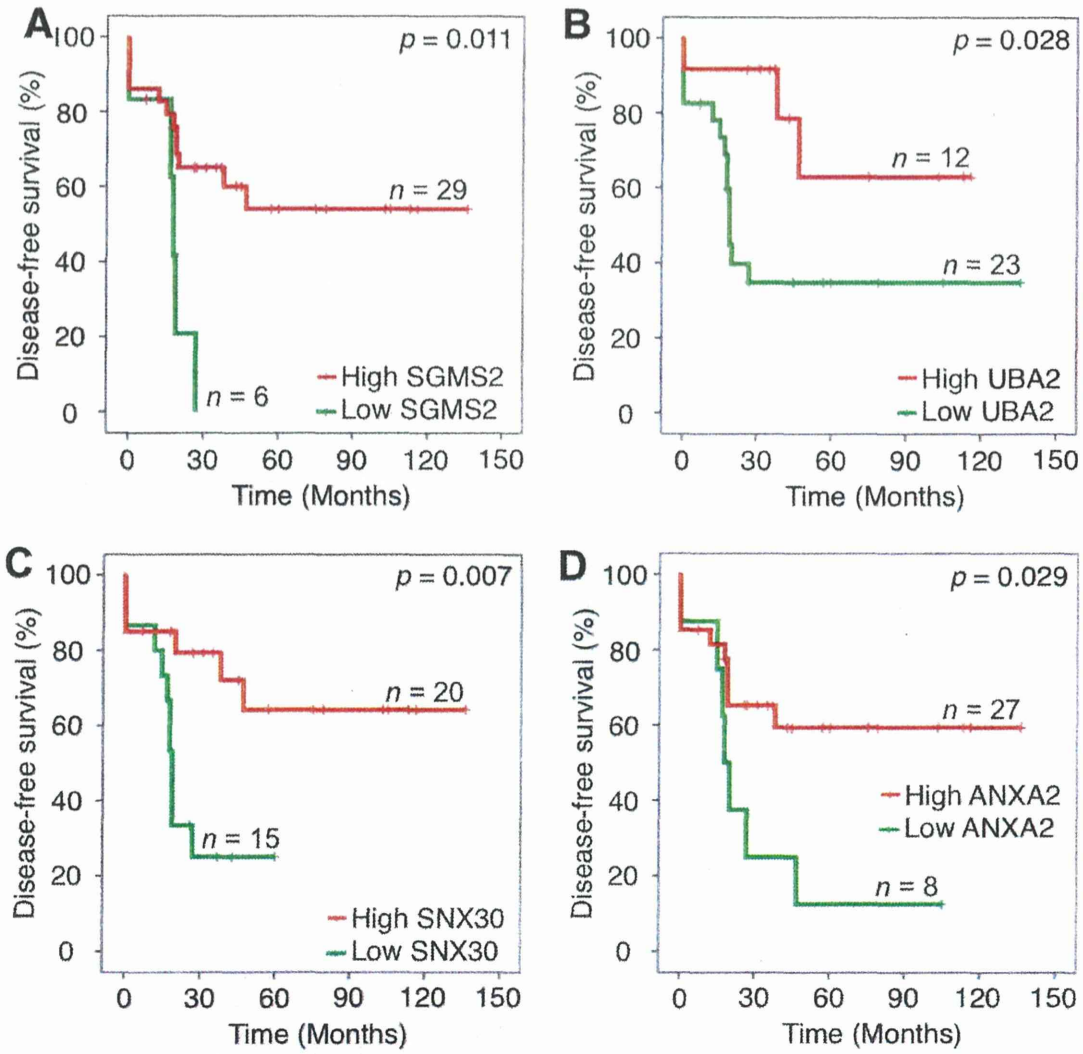

Figure 6. The low expression levels of miR-133a target genes correlate with poor survival of osteosarcoma patients. **(A–D):** Kaplan-Meier survival curves of disease-free survival according to the expression levels of the miR-133a target genes including *SGMS2* (A), *UBA2* (B), *SNX30* (C), *ANXA2* (D) in 35 patient biopsy samples. The optimal cutoff points were determined by the Youden index under the receiver-operating characteristic curve. The statistical significance of differences were determined by the log-rank test. Abbreviations: ANAX2, annexin A2; SGMS2, sphingomyelin synthase 2; SNX30, sorting nexin family member 30; UTR, untranslated region; UBA2, ubiquitin-like modifier activating enzyme 2.

1 showed only a little efficacy on invasiveness in osteosarcoma cells. The most important miRNA that could regulate the multiple phenotypes of osteosarcoma-initiating cells was miR-133a. Although miR-1 and miR-133a correlate with the proliferation of muscle progenitor cells and promote myogenesis [58], their importance in muscle physiology and disease remains unclear [59]. Indeed, miR-133a may be dispensable for the normal development and function of skeletal muscle because skeletal muscle development and function appears unaffected in miR-133a transgenic mice [59]. In this study, silencing of miR-133a had no toxic effect on muscle, including heart and skeletal muscle *in vivo* (Supporting Information Fig. S7E–S7G). Because the upregulation of miR-133a in osteosarcoma cells did not regulate the expression levels of CD133, we determined that it regulated multiple pathways that are not upstream of CD133 expression. Since the inducible factors of CD133 in osteosarcoma have not been cleared, further investigation of the relationship between the tumor microenvironment and CD133 might be warranted. Indeed, the activation of the hypoxia signaling pathway, for example, has been reported to trigger many pathways important for stem cell maintenance [60–62].

Second, we determined the efficacy of LNA technology, an antisense miRNA inhibitor oligonucleotide, as therapeutics against solid cancer. To date, the efficacy of LNAs against human disease has been reported in hepatitis and lymphoma. For example, LNA-antimiR-122 (Miravirsen, Santaris Pharma, San Diego, CA) effectively treats chimpanzees infected with

©AlphaMed Press 2013

hepatitis C virus without any observable resistance or physiological side effects [63]. This treatment has advanced to phase II clinical trials, which emphasizes the strengths of LNA-mediated miR-122 silencing, including high efficacy and good tolerability without adverse effects [64]. The other report represents the preclinical trial of LNA-mediated miR-155 silencing against low-grade B-cell lymphoma [65]. Therefore, our preclinical study contributes to the broad application of LNA treatment including solid tumors. While an effective drug delivery system has been the most challenging remaining consideration for the successful translation of RNAi to the clinic for broad use in patients, the systemic administration of LNA-133a did not need assistance of drug delivery system to decrease the expression of miR-133a. These results are consistent with the results of the trial of LNA against HCV infection, in which the LNA was injected via subcutaneous injection. This preclinical trial will not only provide a novel treatment strategy against osteosarcoma but will also support a wide range of LNA applications against cancers that require the silencing of specific miRNAs.

Third, the multiple targets of miR-133a were identified to have antitumor functions against osteosarcoma with clinical relevance. Using an siRNA-induced gene knockdown system and a 3′ UTR luciferase reporter assay, we identified *SGMS2*, *UBA2*, *SNX30*, and *ANXA2* as novel antitumor molecules of osteosarcoma. Some of these molecules have been reported their association with other cancers but not for osteosarcoma. *SGMS2*, located on 4q25, is an enzyme that catalyzes the conversion of phosphatidylcholine and ceramide to sphingomyelin and diacylglycerol [66]. The specific activation of *SGMS2* explains the ability of this gene to trigger cell cycle arrest, cell differentiation, and autophagy or apoptosis in cancer cells [47]. *UBA2*, located on 19q12, forms a heterodimer that functions as a small ubiquitin-like modifier (SUMO)-activating enzyme for the sumoylation of proteins [67]. Conjugating SUMO-1, one of the four SUMO isoforms, to wild-type p53 increases the transactivation ability of p53 [45]. *SNX30*, located on 9q32, may mediate membrane association either through the lipid-binding PX domain (a phospholipid-binding motif) or protein-protein interactions. Although *SNX30* has not been well studied in cancer, loss of *SNX1*, one of the *SNX* families, plays a significant role in the development and aggressiveness of human colon cancer, at least partially through increased signaling from the endosomes [46]. In this study, we found correlations between the expression of *SGMS2*, *UBA2*, and *SNX30* and osteosarcoma cell invasion, as well as a close correlation with the prognosis of osteosarcoma patients. *ANXA2*, located on 15q22, belongs to a large family of diverse proteins that are characterized by conserved annexin repeat domains and the ability to bind negatively charged phospholipids in a calcium-dependent manner [68]. The expression levels of *ANXA2* are decreased in a subset of human OS metastases and metastatic lines [69], but the actual role of *ANXA2* in suppressing OS metastasis has remained unclear [37], which was identified as a regulator of osteosarcoma cell invasion. In this study, we were unable to identify the target genes of miR-133a that were involved in cellular proliferation, which is a general characteristic of TICs. This result may provide one explanation for why the difference in the proliferation rate of the $CD133^{high}$ and $CD133^{low}$ cell populations was relatively small. Another reason for this difference may have been heterogeneiety even within the $CD133^{high}$ cell population. Further investigation of additional markers might shed further light on the mechanisms underlying these phenotypes.

The most interesting and surprising results were the close correlations between the clinical behaviors of osteosarcoma and the expression of the factors associated with malignant tumor-initiating phenotypes, including CD133, miR-133a, and the target genes of miR-133a. These results support the importance of silencing of miR-133a during osteosarcoma treatment. Indeed, the target molecules of miR-133a were found to be significant and novel prognostic factors for osteosarcoma patients. Further analyses of these factors, including *SGMS2*, *UBA2*, and *SNX30*, would allow a better understanding of the molecular mechanisms that regulate osteosarcoma progression.

Overall, our study represents a novel approach for the use of RNAi therapeutics against the lethal phenotype of osteosarcoma. To the best of our knowledge, this study is the first preclinical trial of RNAi therapy overcoming the sarcoma malignancy. We found that miR-133a, which was induced by chemotherapy treatment, is a key regulator of cell invasion of the malignant cell population within osteosarcoma. In a preclinical *in vivo* experiment, systemic administration of LNA-133a with chemotherapy suppressed the osteosarcoma metastasis via the multiple pathways without any significant toxicity. Silencing of miR-133a may therefore represent a novel therapeutic strategy against osteosarcoma, which would lead to an improvement in the prognosis of osteosarcoma patients.

Conclusion

Silencing of miR-133a reduced the malignancy of $CD133^{high}$ osteosarcoma-initiating cell population through restoring the expression of multiple target genes. Systemic administration of LNA-133a with CDDP reduced lung metastasis and prolonged the survival of osteosarcoma-bearing mice. A clinical study revealed that high miR-133a expression levels within the patient biopsy specimens were significantly correlated with poor prognosis, providing the importance of regulating miR-133a levels in osteosarcoma for more efficient therapy in future.

Acknowledgments

We thank T. Yamada for the cDNA library of osteosarcoma clinical samples. We also thank A. Inoue for her technical work. This work was supported in part by a grant-in-aid for the Third-Term Comprehensive 10-Year Strategy for Cancer Control of Japan, the Program for Promotion of Fundamental Studies in Health Sciences of the National Institute of Biomedical Innovation of Japan (NiBio), and a grant-in-aid for Scientific Research on Applying Health Technology from the Ministry of Health, Labor and Welfare of Japan.

Author contributions

T.F.: performed the experimental work, data analysis, and writing of the draft of the manuscript; T.K., K.H., and Y.Y.:

©AlphaMed Press 2013

provided the technical skills for the *in vitro* assay; N.K. and R.T.: participated in the conception, design, and coordination of the study; F.T.: provided the technical skills for the *in vivo* LNA delivery; D.K., I.K., A.Y., and E.K.: provided osteosarcoma biopsy samples and their information; H.I.: provided osteosarcoma cell lines from clinical samples resected at the National Cancer Center Hospital of Japan. A.K. and T.O.: initiated the project and provided helpful discussion. The manuscript was finalized by T.O. with the assistance of all authors.

Disclosure of Potential Conflicts of Interest

The authors indicate no potential conflicts of interest.

References

1 Aogi K, Woodman A, Urquidi V et al. Telomerase activity in soft-tissue and bone sarcomas. Clin Cancer Res 2000;6:4776–4781.
2 Fletcher CD. The evolving classification of soft tissue tumours: An update based on the new WHO classification. Histopathology 2006;48:3–12.
3 Naka N, Takenaka S, Araki N et al. Synovial sarcoma is a stem cell malignancy. Stem Cells 2010;28:1119–1131.
4 Reya T, Morrison SJ, Clarke MF et al. Stem cells, cancer, and cancer stem cells. Nature 2001;414:105–111.
5 Clarke MF, Dick JE, Dirks PB et al. Cancer stem cells—Perspectives on current status and future directions: AACR Workshop on cancer stem cells. Cancer Res 2006;66: 9339–9344.
6 Clevers H. The cancer stem cell: Premises, promises and challenges. Nat Med 2011;17:313–319.
7 Visvader JE, Lindeman GJ. Cancer stem cells in solid tumours: Accumulating evidence and unresolved questions. Nat Rev Cancer 2008;8:755–768.
8 Allison DC, Carney SC, Ahlmann ER et al. A meta-analysis of osteosarcoma outcomes in the modern medical era. Sarcoma 2012; 2012:704872.
9 Kawaguchi N, Ahmed AR, Matsumoto S et al. The concept of curative margin in surgery for bone and soft tissue sarcoma. Clin Orthop Relat Res 2004:165–172.
10 Gupta A, Meswania J, Pollock R et al. Non-invasive distal femoral expandable endoprosthesis for limb-salvage surgery in paediatric tumours. J Bone Joint Surg 2006;88: 649–654.
11 Bacci G, Rocca M, Salone M et al. High grade osteosarcoma of the extremities with lung metastases at presentation: Treatment with neoadjuvant chemotherapy and simultaneous resection of primary and metastatic lesions. J Surg Oncol 2008;98:415–420.
12 Halldorsson A, Brooks S, Montgomery S et al. Lung metastasis 21 years after initial diagnosis of osteosarcoma: A case report. J Med Case Rep 2009;3:9298.
13 Adhikari AS, Agarwal N, Wood BM et al. CD117 and Stro-1 identify osteosarcoma tumor-initiating cells associated with metastasis and drug resistance. Cancer Res 2010; 70:4602–4612.
14 Basu-Roy U, Seo E, Ramanathapuram L et al. Sox2 maintains self renewal of tumor-initiating cells in osteosarcomas. Oncogene 2012;31:2270–2282.
15 Gibbs CP, Kukekov VG, Reith JD et al. Stem-like cells in bone sarcomas: Implications for tumorigenesis. Neoplasia 2005;7:967–976.
16 Levings PP, McGarry SV, Currie TP et al. Expression of an exogenous human Oct-4 promoter identifies tumor-initiating cells in osteosarcoma. Cancer Res 2009;69:5648–5655.
17 Siclari VA, Qin L. Targeting the osteosarcoma cancer stem cell. J Orthop Surg Res 2010;5:78.
18 Tirino V, Desiderio V, d'Aquino R et al. Detection and characterization of CD133+ cancer stem cells in human solid tumours. PloS one 2008;3:e3469.
19 Tirino V, Desiderio V, Paino F et al. Human primary bone sarcomas contain CD133+ cancer stem cells displaying high tumorigenicity in vivo. FASEB J 2011;25: 2022–2030.
20 Wilson H, Huelsmeyer M, Chun R et al. Isolation and characterisation of cancer stem cells from canine osteosarcoma. Vet J 2008; 175:69–75.
21 Wu C, Wei Q, Utomo V et al. Side population cells isolated from mesenchymal neoplasms have tumor initiating potential. Cancer Res 2007;67:8216–8222.
22 Gregory RI, Shiekhattar R. MicroRNA biogenesis and cancer. Cancer Res 2005;65: 3509–3512.
23 Ambros V. microRNAs: Tiny regulators with great potential. Cell 2001;107:823–826.
24 Calin GA, Croce CM. MicroRNA signatures in human cancers. Nat Rev Cancer 2006;6:857–866.
25 Esquela-Kerscher A, Slack FJ. Oncomirs—MicroRNAs with a role in cancer. Nat Rev Cancer 2006;6:259–269.
26 Ma S, Tang KH, Chan YP et al. miR-130b Promotes CD133(+) liver tumor-initiating cell growth and self-renewal via tumor protein 53-induced nuclear protein 1. Cell Stem Cell 2010;7:694–707.
27 Calin GA, Ferracin M, Cimmino A et al. A MicroRNA signature associated with prognosis and progression in chronic lymphocytic leukemia. New Engl J Med 2005;353:1793–1801.
28 Jiang J, Gusev Y, Aderca I et al. Association of microRNA expression in hepatocellular carcinomas with hepatitis infection, cirrhosis, and patient survival. Clin Cancer Res 2008;14:419–427.
29 Kawai A, Ozaki T, Ikeda S et al. Two distinct cell lines derived from a human osteosarcoma. J Cancer Res Clin Oncol 1989;115: 531–536.
30 Osaki M, Takeshita F, Sugimoto Y et al. MicroRNA-143 regulates human osteosarcoma metastasis by regulating matrix metalloprotease-13 expression. Mol Ther 2011;19:1123–1130.
31 Youden W. Index for rating diagnostic tests. Cancer 1950;3:32–35.
32 Gires O. Lessons from common markers of tumor-initiating cells in solid cancers. Cell Mol Life Sci 2011;68:4009–4022.
33 Cao Y, Zhou Z, de Crombrugghe B et al. Osterix, a transcription factor for osteoblast differentiation, mediates antitumor activity in murine osteosarcoma. Cancer Res 2005;65: 1124–1128.
34 de Crombrugghe B, Lefebvre V, Behringer RR et al. Transcriptional mechanisms of chondrocyte differentiation. Matrix Biol 2000;19:389–394.
35 Ducy P, Zhang R, Geoffroy V et al. Osf2/Cbfa1: A transcriptional activator of osteoblast differentiation. Cell 1997;89:747–754.
36 Nakashima K, Zhou X, Kunkel G et al. The novel zinc finger-containing transcription factor osterix is required for osteoblast differentiation and bone formation. Cell 2002;108: 17–29.
37 Tang N, Song WX, Luo J et al. Osteosarcoma development and stem cell differentiation. Clin Orthop Relat Res 2008;466:2114–2130.
38 Croce CM. Causes and consequences of microRNA dysregulation in cancer. Nat Rev. Genet 2009;10:704–714.
39 Elmen J, Lindow M, Schutz S et al. LNA-mediated microRNA silencing in non-human primates. Nature 2008;452:896–899.
40 Haraguchi T, Nakano H, Tagawa T et al. A potent 2′-O-methylated RNA-based microRNA inhibitor with unique secondary structures. Nucleic Acids Res 2012;40:e58.
41 Obad S, dos Santos CO, Petri A et al. Silencing of microRNA families by seed-targeting tiny LNAs. Nat Genet 2011;43:371–378.
42 Dass CR, Ek ET, Choong PF. Human xenograft osteosarcoma models with spontaneous metastasis in mice: Clinical relevance and applicability for drug testing. J Cancer Res Clin Oncol 2007;133:193–198.
43 Kimura K, Nakano T, Park Y-B et al. Establishment of human osteosarcoma cell lines with high metastatic potential to lungs and their utilities for therapeutic studies on metastatic osteosarcoma. Clin Exp Metastasis 2002;19:477–486.
44 Tsuchida R, Das B, Yeger H et al. Cisplatin treatment increases survival and expansion of a highly tumorigenic side-population fraction by upregulating VEGF/Flt1 autocrine signaling. Oncogene 2008;27:3923–3934.
45 Gostissa M, Hengstermann A, Fogal V et al. Activation of p53 by conjugation to the ubiquitin-like protein SUMO-1. EMBO J 1999; 18:6462–6471.
46 Nguyen LN, Holdren MS, Nguyen AP et al. Sorting nexin 1 down-regulation promotes colon tumorigenesis. Clin Cancer Res 2006;12:6952–6959.

©AlphaMed Press 2013